SEMARAK ILMU PUBLISHING

Semarak International Journal of Mechanical Precision and Engineering

Journal homepage:
https://semarakilmu.my/index.php/sijmpe/index
ISSN: 3083-9546

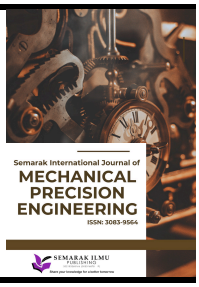

Heimenz Flow Over Shrinking or Stretching Sheet in a Ternary Hybrid Nanofluid

Nur Farisya Mohd Ruslan[1], Nur Hazirah Adilla Norzawary[2], Nur Syahirah Wahid[1,*], Mohd Ezad Hafidz Hafidzuddin[3]

[1] Department of Mathematics and Statistics, Faculty of Science, Universiti Putra Malaysia, 43400 UPM Serdang, Selangor, Malaysia
[2] Institute for Mathematical Research, Universiti Putra Malaysia, 43400 UPM Serdang, Selangor, Malaysia
[3] Centre of Foundation Studies for Agricultural Science, Universiti Putra Malaysia, 43400 UPM Serdang, Selangor, Malaysia

ARTICLE INFO

Article history:
Received 10 October 2024
Received in revised form 7 November 2024
Accepted 25 November 2024
Available online 30 December 2024

Keywords:
Hiemenz flow; ternary hybrid nanofluid; stretching/shrinking sheet; MATLAB

ABSTRACT

The Hiemenz flow over a shrinking or stretching sheet in a ternary hybrid nanofluid is examined in this study. Utilising copper *Cu,* titanium dioxide TiO_2, and alumina Al_2O_3 nanoparticles dissolved in water, the study seeks to figure out the improved heat transfer characteristics of ternary hybrid nanofluids through the considered control parameters. This study investigates the thermal and flow behavior of ternary hybrid nanofluids in various boundary layer configurations. The governing equations are initially formulated as partial differential equations (PDEs) based on the principles of mass, momentum, and energy conservation. These PDEs are then transformed into a system of nonlinear ordinary differential equations (ODEs) using similarity transformations, enabling the analysis of boundary layer flow under specific conditions. These resulting equations subjected to the boundary conditions are then solved numerically by using bvp4c in MATLAB software. This study found that, based on the first solution, a high local Nusselt number can be achieved by increasing the volume fraction of TiO_2 nanoparticles, suggesting that a suitably more concentrated TiO_2 composition could improve the heat transfer rate in the system. Moreover, increasing the volume fraction of TiO_2 could increase the skin friction coefficient. Additionally, delaying boundary layer separation is possible by carefully tuning the stretching or shrinking parameter λ. Specifically, the boundary layer separation occurs when the sheet is shrunk extensively. These discoveries provide important insights for improving heat transfer systems and developing industrial and engineering applications for nanofluids.

1. Introduction

Stagnation-point flows, describing the fluid motion near the stagnation region at the front of a blunt-nosed body, exist on all solid bodies moving in a fluid. The stagnation region encounters the highest pressure, the highest heat transfer, and the highest rates of mass deposition. Hiemenz [1]

* *Corresponding author.*
E-mail address: syahirahwahid@upm.edu.my

https://doi.org/10.37934/sijmpe.1.1.4455a

was the first to study two-dimensional stagnation flows using a similarity transform to reduce the Navier-Stokes equations to nonlinear ordinary differential equations. Hiemenz flow is the stagnation point flow by using similarity of the solution to reduce number of variables by means of coordinate transformation.

The study of boundary layer flow over a stretching or shrinking sheet is a fundamental topic in fluid mechanics, with significant implications for both theoretical research and practical applications. Boundary layer flow refers to the thin region adjacent to the surface where viscous effects are significant, and the analysis of this flow is crucial for understanding heat and mass transfer processes in various engineering systems [2]. Stretching and shrinking sheet problems have garnered considerable attention due to their relevance in industrial applications such as extrusion processes, hot rolling, wire drawing, and glass-fiber production. In these applications, the surface velocity can vary, leading to complex boundary layer behaviors [3]. A stretching sheet typically occurs when a material is pulled, causing it to elongate and thin, while a shrinking sheet involves the material contracting and thickening as it is compressed.

The mathematical modeling of these phenomena often involves solving the Navier-Stokes equations under specific boundary conditions to describe the velocity and temperature fields within the boundary layer. These models are further complicated when considering non-Newtonian fluids, magnetohydrodynamics, or thermal radiation effects, which are essential for accurately predicting the behavior in real-world applications [4].

In recent years, the introduction of nanofluids—fluids containing nanometer-sized particles has added another layer of complexity and interest to the study of boundary layer flows. Nanofluids have enhanced thermal properties, making them highly effective for heat transfer applications [5]. The combination of stretching/shrinking sheet dynamics with nanofluids presents a promising area for enhancing thermal management systems in various high-performance engineering applications.

The study by Waini *et al.,* [6] investigates the Hiemenz flow of a hybrid nanofluid composed of alumina (Al_2O_3) and copper (Cu) nanoparticles over a stretching and shrinking surface. The primary objective is to derive the mathematical correlations for the thermophysical properties of the ternary hybrid nanofluid and hybrid nanofluid. The results indicate that dual solutions exist for several physical parameters and that the stability analysis confirms the stable solution. Zainal *et al.,* [7] investigated the heat generation and absorption effects on the magnetohydrodynamic (MHD) flow of a hybrid nanofluid over a bidirectional exponential stretching and shrinking sheet. The study found that increasing the nanoparticle volume fraction and magnetic parameter enhances the skin friction coefficient, while the suction parameter improves the heat transfer rate. Conversely, the presence of heat generation reduces the heat transfer rate.

In recent research by Zari *et al.,* [8] the study focused on the analysis of Hiemenz flow towards a stretching Riga plate in a hybrid nanofluid medium comprising alumina (Al_2O_3) and copper (Cu) nanoparticles dispersed in water (H_2O), with the combined effects of thermal radiation, viscous dissipation, and joule heating. The findings indicate that the incorporation of electromagnetic and thermal radiation effects can substantially improve the performance of hybrid nanofluids in heat transfer applications. Reddy *et al.,* [9] investigated the heat and mass transfer characteristics of hybrid nanofluid flow over a stretching or shrinking sheet, incorporating the effects of slip, chemical reactions, suction, and thermal radiation. The hybrid nanofluid comprised water as the base fluid and a combination of Alumina (Al_2O_3) and Titanium Oxide (TiO_2) nanoparticles. The study revealed that the temperature of the hybrid nanofluid increased with higher volume fractions of nanoparticles in both steady and unsteady cases. A considerable amount of research has also been carried out on this subject by other researchers, as evidenced by studies [10-14].

The study aspects of non-unique solutions for hiemenz flow filled with ternary hybrid nanofluid over a stretching/shrinking sheet by Jamrus *et al.,* [15] investigates the behavior of hiemenz flow involving a ternary hybrid nanofluid across a stretching/shrinking sheet. The results indicate that skin friction values are significantly affected by the magnitude of the stretching/shrinking parameter, and that the heat conduction efficiency of the ternary hybrid nanofluid surpasses that of the hybrid nanofluid. Notably, within a specific range of the shrinking/stretching parameter, the system exhibits two distinct solutions, with stability analysis revealing that only one solution remains stable over time.

Jamrus *et al.,* [16] focused on the laminar magnetohydrodynamic (MHD) flow of a ternary hybrid nanofluid over a permeable stretching sheet with suction and magnetic field effects. Their findings indicated that while unsteadiness and suction parameters enhance the heat transfer rate, the magnetic parameter reduces it, providing critical insights for optimizing thermal systems involving hybrid nanofluids.

However, despite the growing interest in hybrid nanofluids, studies specifically addressing Hiemenz flow over shrinking or stretching sheets in a ternary hybrid nanofluid remain scarce. To the best of our knowledge, no comprehensive study has been conducted on this specific topic, highlighting a significant research gap. Ternary hybrid nanofluids, which incorporate three different nanoparticles, have received relatively little attention compared to conventional hybrid or mono nanofluids. The limited research in this area presents an opportunity to explore the effects of ternary hybrid nanofluids in enhancing heat and mass transfer performance, offering potential advantages in engineering applications.

Ternary hybrid nanofluids have gained significant attention for their advanced thermal and rheological properties, making them highly relevant to precision engineering applications. Research has focused on optimizing their thermophysical properties using advanced methods like neural networks and response surface methodology to enhance thermal conductivity and viscosity [17]. Their flow behavior and heat transfer capabilities have been explored in various scenarios, such as through stenosed arteries [18] and over stretching sheets [19], providing insights into their potential for precise fluid control in industrial and biomedical systems. Studies have also reported the synthesis and characterization of novel ternary hybrid nanoparticles, including metal-metal-oxide-carbon combinations, which offer superior thermal performance [20]. These findings collectively highlight the applicability of ternary hybrid nanofluids in enhancing thermal management, lubrication, and energy efficiency in high-precision engineering processes [21].

2. Methodology

The Hiemenz flow of a ternary hybrid nanofluid on a stretching/shrinking surface is considered. The flow configuration of the problem is illustrated in Figure 1. Here, the free stream velocity is taken as $u_e(x) = U_e(x)$, while the surface velocity is $u_w(x) = U_w(x)$ with U_e and U_w are constants. The ambient T_∞ and the surface T_w temperatures are also constants.

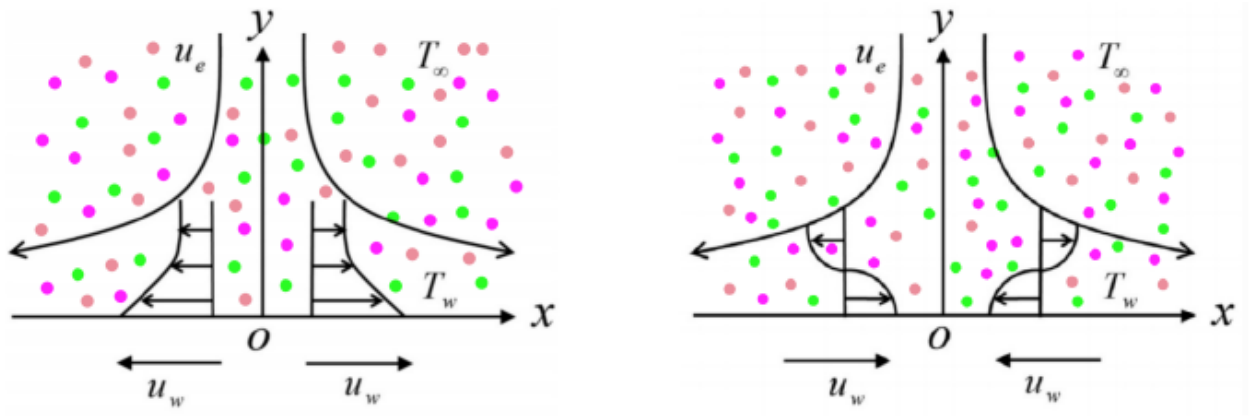

(a) (b)

Fig. 1. Comparison of (a) stretching and (b) shrinking surface

Therefore, the governing equations are [6,22-24]:

$$\frac{\partial u}{\partial x}+\frac{\partial v}{\partial y}=0, \tag{1}$$

$$u\frac{\partial u}{\partial x}+v\frac{\partial u}{\partial y}=u_e\frac{du_e}{dx}+\frac{\mu_{thnf}}{\rho_{thnf}}\frac{\partial^2 u}{\partial y^2}, \tag{2}$$

$$u\frac{\partial T}{\partial x}+v\frac{\partial T}{\partial y}=\frac{k_{thnf}}{(\rho C_p)_{thnf}}\frac{\partial^2 T}{\partial y^2}, \tag{3}$$

$$\begin{aligned} &u=u_w(x),\ v=0,\ T=T_w \ \text{ at } \ y=0,\\ &u\to u_e(x),\ \ T\to T_\infty \ \text{ as } \ y\to\infty \end{aligned} \tag{4}$$

where (u,v) are the velocity component along (x,y) – axes, and T is the temperature of the tetra-hybrid nanofluid. Further, μ_{thnf} is the dynamic viscosity, ρ_{thnf} is the density, k_{thnf} is the conductivity and $\left(\rho C_p\right)_{thnf}$ is the heat capacity, of the tetra-hybrid nanofluid which the formulations are provided in Table 1. Note that *Al₂O₃* (ϕ_1), *Cu* (ϕ_2) and *TiO₂* (ϕ_3) are the nanoparticles used in this study, with their thermophysical properties values tabulated in Table 2.

Table 1
The model of thermophysical properties

Properties	Model
Dynamic viscosity	$\mu_{thnf} = \dfrac{\mu_f}{(1-\phi_1)^{2.5}(1-\phi_2)^{2.5}(1-\phi_3)^{2.5}}$
Density	$\rho_{thnf} = (1-\phi_3)\left((1-\phi_3)\left((1-\phi_2)\left((1-\phi_1)\rho_f + \phi_1\rho_1\right) + \phi_2\rho_2\right) + \phi_3\rho_3\right)$
Heat capacitance	$(\rho C_p)_{thnf} = (1-\phi_3)\left((1-\phi_2)\left((1-\phi_1)(\rho C_p)_f + \phi_1(\rho C_p)_1\right) + \phi_2(\rho C_p)_2\right) + \phi_3(\rho C_p)_3$
Thermal conductivity	$k_{thnf} = \dfrac{k_3 + 2k_{hnf} - 2\phi_3(k_{hnf} - k_3)}{k_3 + 2k_{hnf} + \phi_3(k_{hnf} - k_3)} \times k_{hnf}$ where $k_{hnf} = \dfrac{k_2 + 2k_{nf} - 2\phi_2(k_{nf} - k_2)}{k_2 + 2k_{nf} + \phi_2(k_{nf} - k_2)} \times k_{nf}$ $k_{nf} = \dfrac{k_1 + 2k_f - 2\phi_1(k_f - k_1)}{k_1 + 2k_f + \phi_1(k_f - k_1)} \times k_f$

Table 2
Value of thermophysical properties

Properties	H_2O	Al_2O_3	Cu	TiO_2
$\rho(\mathrm{kg/m^3})$	997.1	3970	8933	4250
$C_p(\mathrm{J/kgK})$	4179	765	385	686.2
$k(\mathrm{W/mK})$	0.613	40	400	8.9538
Pr	6.2			

Next, similarity variables are introduced, such that [25]:

$$\psi = \left(U_e \nu_f\right)^{1/2} f(\eta),\ \theta(\eta) = \frac{T - T_\infty}{T_w - T_\infty},\ \eta = y\sqrt{\frac{U_e}{\nu_f}} \tag{5}$$

By applying the similarity variables from Eq. (4) to Eqs. (2) and (3), the model reduces to the following boundary value problems in the form of ODEs, such that:

$$\left(\frac{\mu_{thnf}/\mu_f}{\rho_{thnf}/\rho_f}\right) f''' + ff'' + 1 - f'^2 = 0, \tag{6}$$

$$\frac{1}{\mathrm{Pr}}\left(\frac{k_{thnf}/k_f}{(\rho C_p)_{thnf}/(\rho C_p)_f}\right)\theta'' + f\theta' = 0, \tag{7}$$

$$\begin{aligned} &f(0) = 0,\ f'(0) = \lambda,\ \theta(0) = 1, \\ &f'(\infty) \to 0,\ \theta(\infty) \to 0 \end{aligned} \tag{8}$$

where the involved dimensionless parameters are Prandtl number $\mathrm{Pr}=\left(\mu C_p\right)_f / k_f$, stretching/shrinking parameter $\lambda=\frac{U_w}{U_e}$, where $\lambda>0$ for stretching, $\lambda<0$ for shrinking and $\lambda=0$ for static sheet.

The interest physical quantities, specifically the skin friction coefficient C_f and the local Nusselt number Nu_x, defined as follows:

$$C_f=\frac{\mu_{thnf}}{\rho_f u_e^2(x)}\left(\frac{\partial u}{\partial y}\right)_{y=0},\ Nu_x=\frac{x k_{thnf}}{k_f\left(T_w-T_\infty\right)}\left(-\frac{\partial T}{\partial y}\right)_{y=0} \tag{9}$$

Using Eq. (4), Eq. (8) transforms to:

$$\mathrm{Re}_x^{1/2} C_f=\frac{\mu_{thnf}}{\mu_f} f''(0),\ \mathrm{Re}_x^{-1/2} Nu_x=-\frac{k_{thnf}}{k_f}\theta'(0) \tag{10}$$

where $\mathrm{Re}_x=U_e x / \nu_f$ is the local Reynolds number.

3. Results

The classical Hiemenz problem is recovered when the nanoparticle volume fractions $\phi_1=\phi_2=\phi_3=0$(representing a regular fluid) and the stretching or shrinking parameter $\lambda=0$ (indicating a rigid surface). Under these conditions, the calculated value of $f''=1.2325587654$. This result is consistent with the findings of Waini *et al.,* [6] .Additionally, Table 3 presents a comparison of $f''(0)$ values for various cases of λ with $\phi_1=\phi_2=\phi_3=0$, further validating the accuracy of the current results. The current results align well with the referenced literature. Fur- thermore, the calculated values of $\mathrm{Re}_x^{1/2} C_f$ and $\mathrm{Re}_x^{-1/2} Nu_x$ for various parameters, with $\mathrm{Pr}=6.2$, are summarized in Table 4 and this result is also validated with Waini *et al.,* [6].

Table 3
Comparison values of $f''(0)$ with different λ for regular fluid with $\phi_1=\phi_2=\phi_3=0$

λ	Present Results	Waini *et al.,* [6]
2	-1.887306670	-1.887307
1	0	0
0.5	0.713294954	0.713295
0	1.232587654	1.232588
-0.5	1.495669765	1.495670
-1	1.328816875	1.328817
-1.15	1.082231140	1.082231
	[0.116702109]	[0.116702]
-1.2	0.932473323	0.932473
	[0.233649675]	[0.233650]
-1.2465	0.584281373	0.584281
	[0.554296309]	[0.554296]

Note: [ ] Second solution

Table 4

Comparison values of $\mathrm{Re}_x^{1/2} C_f$ and $\mathrm{Re}_x^{-1/2} Nu_x$ for various values of ϕ_1, ϕ_2 and λ with $\phi_3 = 0$

ϕ_2	λ	$\phi_1 = 0$ (*Cu*/water)		$\phi_1 = 0.05$ (*Al₂O₃-Cu*/water)	
		$\mathrm{Re}_x^{1/2} C_f$	$\mathrm{Re}_x^{-1/2} Nu_x$	$\mathrm{Re}_x^{1/2} C_f$	$\mathrm{Re}_x^{-1/2} Nu_x$
0	0	1.232587654	1.127964359	1.408762990	1.229274834
		[1.232588]	[1.127964]	[1.404763]	[1.229275]
0.03		1.425109993	1.213918326	1.605715174	1.317394632
		[1.425110]	[1.213918]	[1.605715]	[1.317395]
0.05		1.553849594	1.269379144	1.738636824	1.374809947
		[1.553850]	[1.269379]	[1.738637]	[1.374810]
0.05	-0.5	1.885501489	0.706314054	2.109729497	0.791230808
		[1.885501]	[0.706314]	[2.109729]	[0.791231]
0	0	1.553849594	1.269379144	1.738636824	1.374809947
		[1.553850]	[1.269379]	[1.738637]	[1.374810]
0.5		0.899208322	1.733859220	1.006144165	1.856884594
		[0.899208]	[1.733859]	[1.006144]	[1.856885]

Note: [ ] Results by Waini *et al.,* [6]

Figure 2 and 3 show result with $\mathrm{Re}_x^{1/2} C_f$ and $\mathrm{Re}_x^{-1/2} Nu_x$ vary for $\phi_3 = 0.01, 0.015, 0.02$ against λ when $\phi_1 = \phi_2 = 0.05$ and $\mathrm{Pr} = 6.2$. According to the results, when ϕ_3 increases, the surface friction increases for $\lambda < 1$ and zero skin friction is noticed when $\lambda = 1$, which align with the tabulation in Table 3. In addition, when ϕ_3 increases, the heat transfer rate increases as the local Nusselt number increases (see Figure 3). The point of bifurcation for different ϕ_3 is the same for all which implies that the concentration of *TiO₂* does not affect the boundary layer separation and this parameter cannot be used to control the flow phase or the separation of boundary layer, where $\lambda_c = -1.2465$. Based on Figure 3, for $\lambda > -1$, the solution of the local Nusselt number is unique.

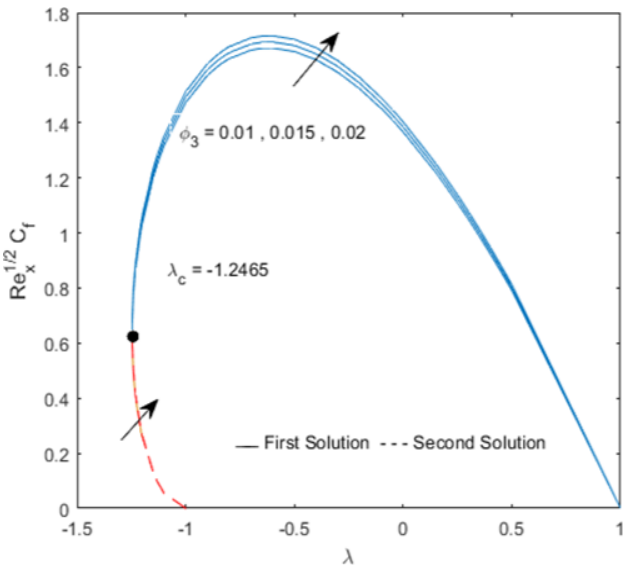

Fig. 2. $\mathrm{Re}_x^{1/2} C_f$ against λ for varies ϕ_3

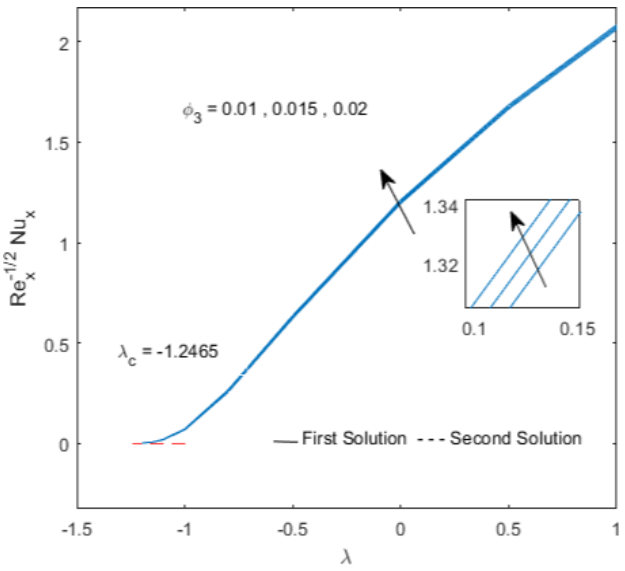

Fig. 3. $\mathrm{Re}_x^{-1/2} Nu_x$ against λ for varies ϕ_3

Further, the velocity $f'(\eta)$ and temperature $\theta(\eta)$ profiles are shown in Figures 4 and 5 for $\phi_3 = 0.01, 0.015, 0.02$ when $\phi_1 = \phi_2 = 0.01$, $\lambda = -1.2$ (for shrinking case) and $\mathrm{Pr} = 6.2$. The findings indicate that while an increase in ϕ_3 reduces the temperature profiles $\theta(\eta)$, it increases the velocity

profiles $f'(\eta)$ for both solution branches. For Figure 4, momentum boundary layer thickness decreases for both solution while for Figure 5 the thermal boundary layer thickness also decreases for both solutions.

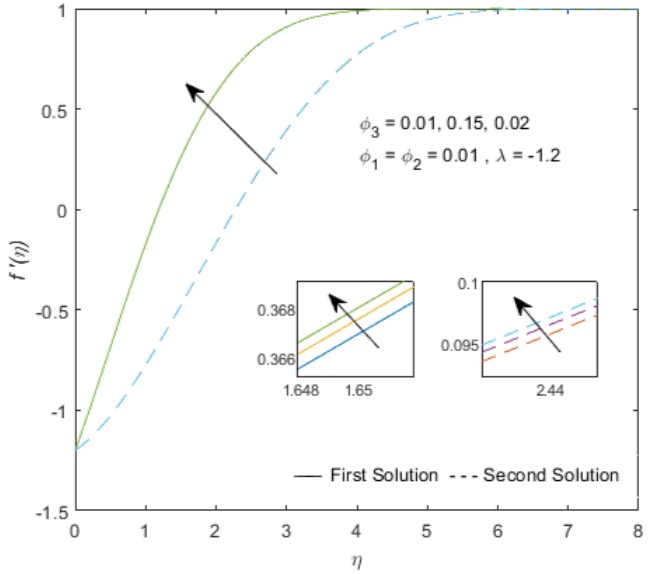

Fig. 4. Effect of ϕ_3 on $f'(\eta)$ (shrinking)

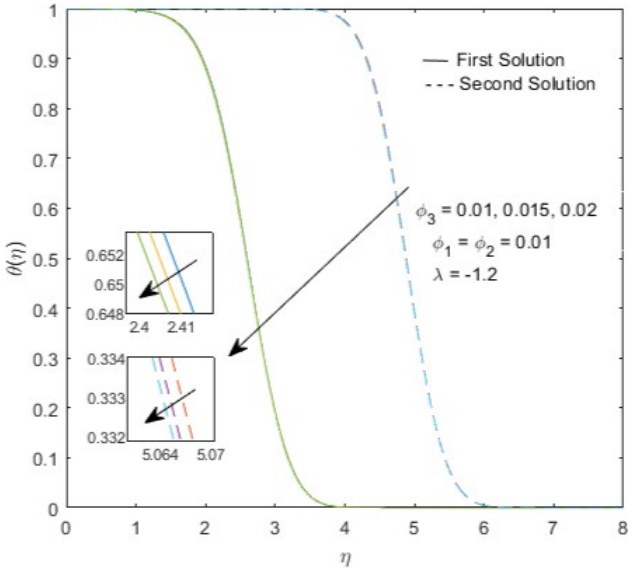

Fig. 5. Effect of ϕ_3 on $\theta(\eta)$ (shrinking)

However, for Figures 6 and 7, when $\lambda = 1.2$ (for stretching case), only the first solution branch was able to be generated. The results reveal that as ϕ_3 increases from 0.01 to 0.02 while maintaining $\phi_1 = \phi_2 = 0.01$ and $\Pr = 6.2$, it reduces velocity of the fluid and thinning the momentum boundary layer thickness for both solution (Figure 6). Meanwhile, the temperature profile increases in Figure 7, and thickening the boundary layer thickness for both solution when ϕ_3 increases.

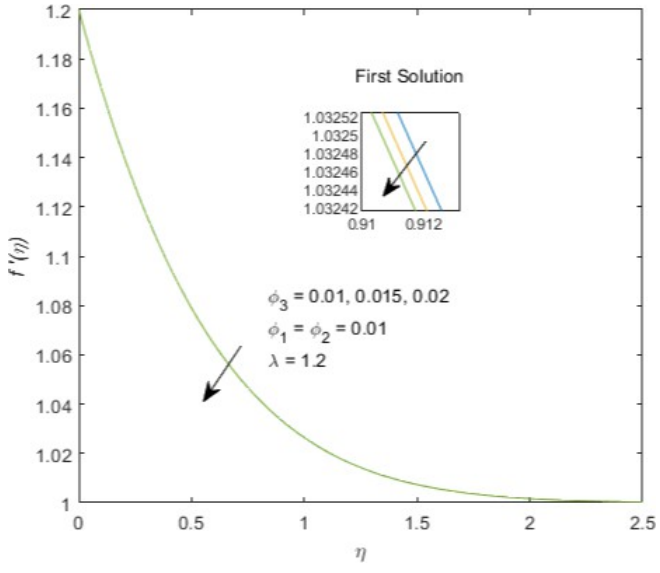

Fig. 6. Effect of ϕ_3 on $f'(\eta)$ (stretching)

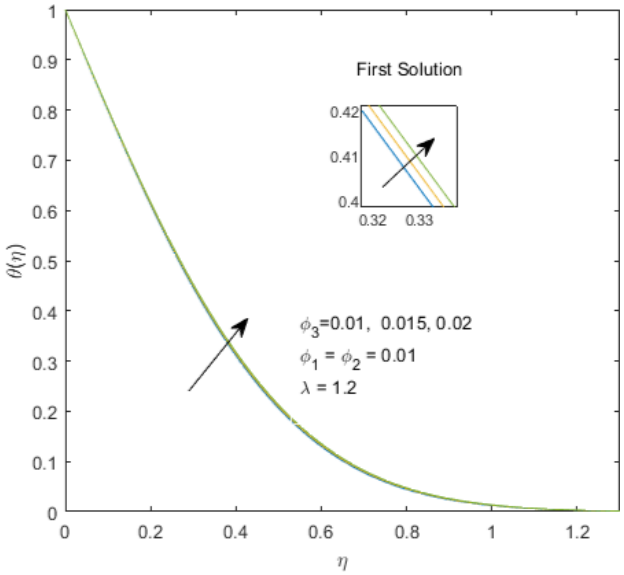

Fig. 7. Effect of ϕ_3 on $\theta(\eta)$ (stretching)

On the other hand, the effect of λ on $f'(\eta)$ and $\theta(\eta)$ when $\phi_1 = \phi_2 = \phi_3 = 0.01$ and $\Pr = 6.2$ are shown in Figures 8 and 9 for shrinking case, ($\lambda < 0$). Based on the first solution in Figure 8, when λ goes from −1.2 to −1.15 and to −1.1, the velocity of the fluid increases and the momentum boundary

layer thickness becomes thinner. Meanwhile, for the second solution, the velocity decreases while thickening the momentum boundary layer thickness. Next, based on the first solution in Figure 9, when λ goes from −1.2 to −1.15 and to −1.1, the temperature of the fluid increases and the thermal boundary layer thickness becomes thickness. Meanwhile, for the second solution, the temperature decreases while the momentum boundary layer thickness.

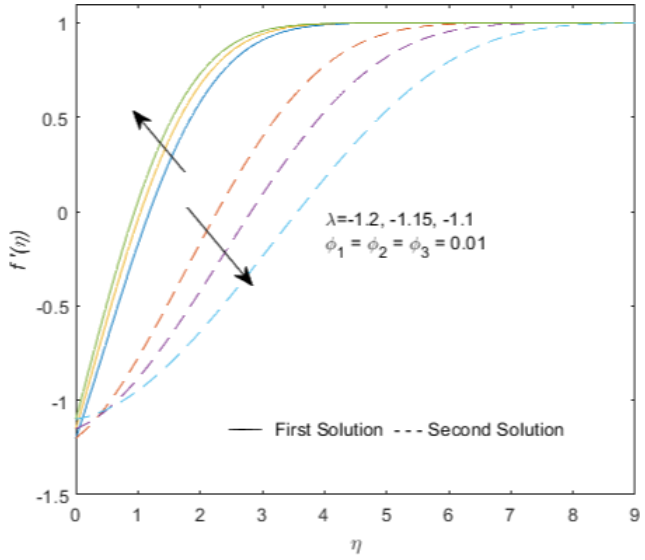

Fig. 8. Effect of shrinking $\lambda < 0$ on $f'(\eta)$

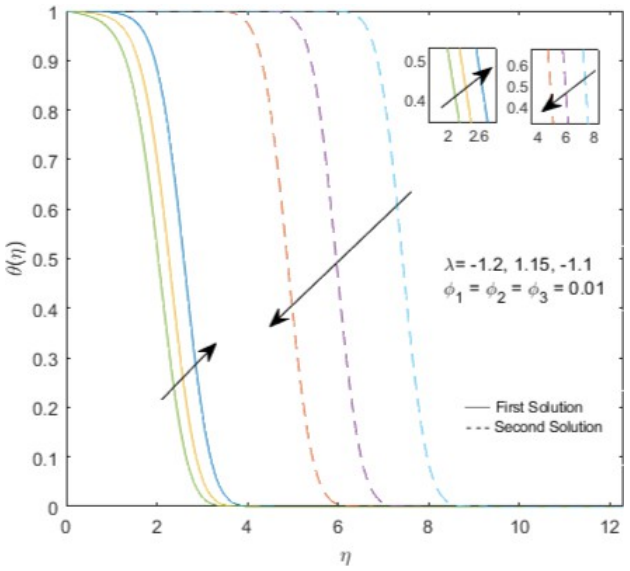

Fig. 9. Effect of shrinking $\lambda < 0$ on $\theta(\eta)$

Meanwhile, for stretching case, only first solution result was taken which can be seen in Figures 10 and 11. When λ increase from 1 to 2 to 3 it shown stretching intensity increase, sheet became more expanding for both Figure 10 and 11. Due to this condition, the velocity profile and the momentum boundary layer increase as can be seen in Figure 10. Meanwhile for Figures 11, the temperature profile decreases and the thermal boundary layer also decreases when the stretching intensity increases.

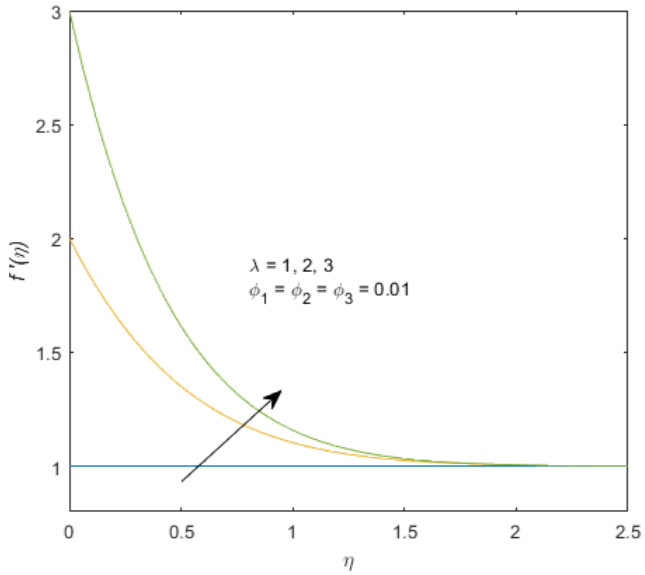

Fig. 10. Effect of stretching $\lambda > 0$ on $f'(\eta)$

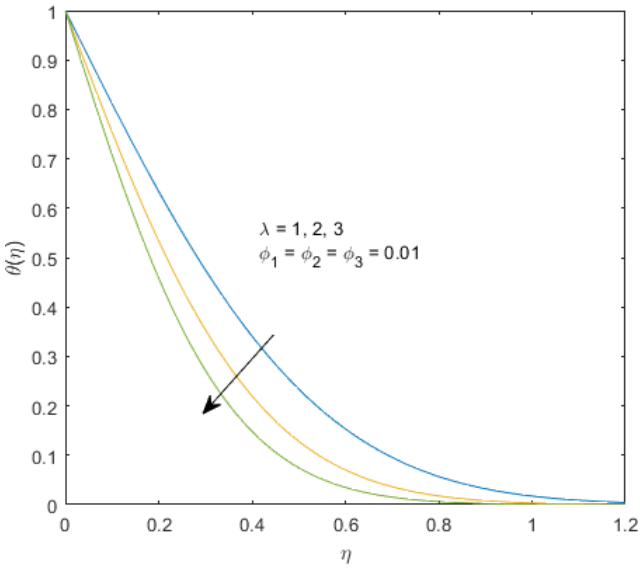

Fig. 11. Effect of stretching $\lambda > 0$ on $\theta(\eta)$

4. Conclusions

The research explores the behavior of Hiemenz flow over a stretching or shrinking sheet immersed in a ternary hybrid nanofluid, focusing on the effects of nanoparticle volume fractions and stretching or shrinking parameters. A mathematical model was formulated and simplified using similarity transformations, and were then solved numerically. The key findings include the identification of dual numerical solutions, particularly in shrinking cases, which highlight the presence of a critical bifurcation point ($\lambda_c = -1.2465$). This bifurcation serves as an indicator of flow stability and transition. Based on the first solution, the flow model can be controlled as follows (see Tables 5 and 6):

Table 5
Flow control suggestions using nanoparticle volume fraction (TiO_2)

Sheet Condition	Physical Quantities	Increment of TiO_2 volume fraction ϕ_3
Shrinking	Skin friction	Increase
	Heat transfer	Increase
	Velocity	Increase
	Temperature	Decrease
Stretching	Skin friction	Increase
	Heat transfer	Increase
	Velocity	Decrease
	Temperature	Increase

Table 6
Flow control suggestions using stretching or shrinking parameter

Physical Quantities	Increment in stretching intensity $\lambda > 0$	Increment in shrinking intensity $\lambda < 0$
Skin friction	Decrease	Increase (until critical point)
Heat transfer	Increase	Decrease
Velocity	Increase	Decrease
Temperature	Decrease	Decrease

Moreover, the bifurcation of the boundary layer is uncontrollable through the adjustment in the volume fraction of TiO_2. It is also believed that the first solution is the most reliable since the previous study by Waini *et al.,* [6] has proven that the first solution is stable compared to the second solution.

Acknowledgement
The authors acknowledged Universiti Putra Malaysia for the given Putra Grant [GP-IPM 9787700].

References
[1] Hiemenz, Karl. "Die Grenzschicht an einem in den gleichformigen Flussigkeitsstrom eingetauchten geraden Kreiszylinder." *Dinglers Polytech. J.* 326 (1911): 321-324.
[2] Schlichting, Hermann, and Klaus Gersten. *Boundary-layer theory*. springer, 2016. https://doi.org/10.1007/978-3-662-52919-5
[3] Crane, Lawrence J. "Flow past a stretching plate." *Zeitschrift für angewandte Mathematik und Physik ZAMP* 21 (1970): 645-647. https://doi.org/10.1007/BF01587695
[4] Andersson, H. I. "MHD flow of a viscoelastic fluid past a stretching surface." *Acta Mechanica* 95, no. 1 (1992): 227-230. https://doi.org/10.1007/BF01170814

[5] Choi, S. US, and Jeffrey A. Eastman. *Enhancing thermal conductivity of fluids with nanoparticles*. No. ANL/MSD/CP-84938; CONF-951135-29. Argonne National Lab.(ANL), Argonne, IL (United States), 1995.
[6] Waini, Iskandar, Anuar Ishak, and Ioan Pop. "Hiemenz flow over a shrinking sheet in a hybrid nanofluid." *Results in Physics* 19 (2020): 103351. https://doi.org/10.1016/j.rinp.2020.103351
[7] Zainal, Nurul Amira, Roslinda Nazar, Kohilavani Naganthran, and Ioan Pop. "Heat generation/absorption effect on MHD flow of hybrid nanofluid over bidirectional exponential stretching/shrinking sheet." *Chinese Journal of Physics* 69 (2021): 118-133. https://doi.org/10.1016/j.cjph.2020.12.002
[8] Zari, Islam, Fatima Ali, Tahir Saeed Khan, and Anum Shafiq. "Radiative Hiemenz flow towards a stretching Riga plate in hybrid nanofluid." *International Communications in Heat and Mass Transfer* 139 (2022): 106492. https://doi.org/10.1016/j.icheatmasstransfer.2022.106492
[9] Reddy, Vivek Y., Edward P. Gerstenfeld, Andrea Natale, William Whang, Frank A. Cuoco, Chinmay Patel, Stavros E. Mountantonakis et al. "Pulsed field or conventional thermal ablation for paroxysmal atrial fibrillation." *New England Journal of Medicine* 389, no. 18 (2023): 1660-1671. https://doi.org/10.1056/NEJMoa2307291
[10] Lanjwani, Hazoor Bux, Muhammad Saleem Chandio, Kamran Malik, and Muhammad Mujtaba Shaikh. "Stability analysis of boundary layer flow and heat transfer of Fe2O3 and Fe-water base nanofluid over a stretching/shrinking sheet with radiation effect." *Engineering, Technology & Applied Science Research* 12, no. 1 (2022): 8114-8122. https://doi.org/10.48084/etasr.4649
[11] Mahabaleshwar, U. S., Emad H. Aly, and T. Anusha. "MHD slip flow of a Casson hybrid nanofluid over a stretching/shrinking sheet with thermal radiation." *Chinese Journal of Physics* 80 (2022): 74-106. https://doi.org/10.1016/j.cjph.2022.06.008
[12] Ibrahim, Muhammad Hafiezul Ridhwan, and Fazlina Aman. "Analysis on Hiemenz flow over a shrinking sheet in hybrid nanofluid." *Enhanced Knowledge in Sciences and Technology* 2, no. 1 (2022): 221-230.
[13] Dero, Sumera, T. N. Abdelhameed, Kamel Al-Khaled, Liaquat Ali Lund, Sami Ullah Khan, and Iskander Tlili. "Contribution of suction phenomenon and thermal slip effects for radiated hybrid nanoparticles (Al 2 O 3− Cu/H 2 O) with stability framework." *International Journal of Modern Physics B* 37, no. 15 (2023): 2350147. https://doi.org/10.1142/S0217979223501473
[14] Kho, Yap Bing, Rahimah Jusoh, Mikhail Sheremet, Mohd Zuki Salleh, Zulkhibri Ismail, and Nooraini Zainuddin. "Unsteady Hiemenz flow of Cu-SiO2 hybrid nanofluid with heat generation/absorption." *Journal of Advanced Research in Fluid Mechanics and Thermal Sciences* 110, no. 2 (2023): 95-107. https://doi.org/10.37934/arfmts.110.2.95107
[15] Jamrus, Farah Nadzirah, Anuar Ishak, Iskandar Waini, Umair Khan, Md Irfanul Haque Siddiqui, and J. K. Madhukesh. "Aspects of Non-unique Solutions for Hiemenz Flow Filled with Ternary Hybrid Nanofluid over a Stretching/Shrinking Sheet." *Advances in Mathematical Physics* 2024, no. 1 (2024): 7253630. https://doi.org/10.1155/2024/7253630
[16] Jamrus, Farah Nadzirah, Iskandar Waini, and Anuar Ishak. "Time-Depending Flow of Ternary Hybrid Nanofluid Past a Stretching Sheet with Suction and Magnetohydrodynamic (MHD) Effects." *Journal of Advanced Research in Fluid Mechanics and Thermal Sciences* 117, no. 2 (2024): 15-27. https://doi.org/10.37934/arfmts.117.2.1527
[17] Hai, Tao, Ali Basem, As' ad Alizadeh, Pradeep Kumar Singh, Husam Rajab, Chemseddine Maatki, Nidhal Becheikh, Lioua Kolsi, Narinderjit Singh Sawaran Singh, and H. Maleki. "Optimizing ternary hybrid nanofluids using neural networks, gene expression programming, and multi-objective particle swarm optimization: a computational intelligence strategy." *Scientific Reports* 15, no. 1 (2025): 1986. https://doi.org/10.1038/s41598-025-85236-3
[18] Hussain Shah, Syed Zahir, Assad Ayub, Umair Khan, Adil Darvesh, El-Sayed M. Sherif, and Ioan Pop. "Thermal transport exploration of ternary hybrid nanofluid flow in a non-Newtonian model with homogeneous-heterogeneous chemical reactions induced by vertical cylinder." *Advances in Mechanical Engineering* 16, no. 5 (2024): 16878132241252229. https://doi.org/10.1177/16878132241252229
[19] Algehyne, Ebrahem A., Haifaa F. Alrihieli, Muhammad Bilal, Anwar Saeed, and Wajaree Weera. "Numerical approach toward ternary hybrid nanofluid flow using variable diffusion and non-Fourier's concept." *ACS omega* 7, no. 33 (2022): 29380-29390. https://doi.org/10.1021/acsomega.2c03634
[20] Zayan, Jalal Mohammed, Abdul Khaliq Rasheed, Akbar John, Waleed Fekry Faris, Abdul Aabid, Muneer Baig, and Batoul Alallam. "Synthesis and characterization of novel ternary-hybrid nanoparticles as thermal additives." *Materials* 16, no. 1 (2022): 173. https://doi.org/10.3390/ma16010173
[21] Priyadharshini, P., M. Vanitha Archana, Nehad Ali Shah, and Mansoor H. Alshehri. "Ternary hybrid nanofluid flow emerging on a symmetrically stretching sheet optimization with machine learning prediction scheme." *Symmetry* 15, no. 6 (2023): 1225. https://doi.org/10.3390/sym15061225
[22] Ariel, P. D. "Hiemenz flow in hydromagnetics." *Acta Mechanica* 103, no. 1 (1994): 31-43. https://doi.org/10.1007/BF01180216

[23] Tiwari, Raj Kamal, and Manab Kumar Das. "Heat transfer augmentation in a two-sided lid-driven differentially heated square cavity utilizing nanofluids." *International Journal of heat and Mass transfer* 50, no. 9-10 (2007): 2002-2018. https://doi.org/10.1016/j.ijheatmasstransfer.2006.09.034

[24] Devi, SP Anjali, and S. Suriya Uma Devi. "Numerical investigation of hydromagnetic hybrid Cu–Al2O3/water nanofluid flow over a permeable stretching sheet with suction." *International Journal of Nonlinear Sciences and Numerical Simulation* 17, no. 5 (2016): 249-257. https://doi.org/10.1515/ijnsns-2016-0037

[25] White, Frank M., and Joseph Majdalani. *Viscous fluid flow*. Vol. 3. New York: McGraw-Hill, 2006.